ChemComm

Accepted Manuscript

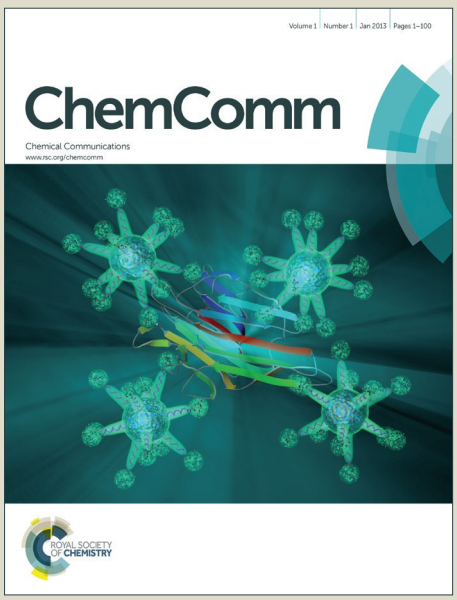

ROYAL SOCIETY OF CHEMISTRY

www.rsc.org/chemcomm

Journal Name

COMMUNICATION

A nanocluster beacon based on the template transformation of DNA-templated silver nanoclusters

Received 00th January 20xx,
Accepted 00th January 20xx

DOI: 10.1039/x0xx00000x

www.rsc.org/

Ye Teng, ‡[ab] Xiaofang Jia, ‡[a] Shan Zhang, [ab] Jinbo Zhu [ab] and Erkang Wang*[a]

In this work, we developed a novel light-up nanocluster beacon (NCB) based on shuttling dark silver nanoclusters (NCs) to bright scaffold through hybrization. The fluorescence enhancement was as high as 70-fold when the two templates were on the opposite sides of the duplexes, enabled sensitive and selective detection of DNA.

Sequence-specific detection of nucleic acids is crucial to genetics[1] and disease diagnostic.[2] Among the numerous strategies for nucleic acid analysis, fluorescence activated upon hybridization with target nucleic acid analytes is of particular interest, which enables the detection without separation and greatly improves signal-to-background ratio. Particularly, molecular beacons as one of the most successful fluorescent probes, are widely used in biomolecular recognition.[3] However, they always suffer from the high cost of labeling and purification, low fluorescence enhancement upon activation and the high background fluorescence from fluctuation of hairpin structures. In response, it is highly desirable for developing low-cost activatable probes to meet the demands in biosensing.

DNA-templated silver nanoclusters (DNA-Ag NCs),[4] as a new class of promising fluorescent nanomaterials, are extensively used in biosensing[5-7] and bioimaging[8, 9] due to their excellent photophysical property, low-cost and good biocompatibility. Moreover the emission wavelength of DNA-Ag NCs can be altered from blue-green to near-infrared spectral region by simply adjusting the base sequence of the template.[10] Recently, Yeh etc. reported a nanocluster beacon (NCB) utilizing DNA-Ag NCs and G-rich sequence.[11] When Ag NCs approached the G-rich sequence through hybridization, the dark Ag NCs would lighted up with a bright red emission. Together with the convenient synthesis and the excellent properties, NCBs were widely used in the construction of sensing platforms for a lot of biomolecules.[12-14] For instance, Yeh etc. developed a chameleon NCB for single-nucleotide polymorphisms detection, which had a 60-70 nm emission shift dependent on the alignment between Ag NCs and G-rich sequences.[15] Nevertheless, the scarcity of flexible and effective methods for modulating the fluorescence of DNA-Ag NCs impedes the development of general biosensors based on DNA-Ag NCs.

In this work, we developed a novel light-up NCB based on shuttling dark DNA-Ag NCs to bright DNA-Ag NCs scaffold. When two DNA templates went in proximity upon hybridization, the dark Ag NCs would transfer to the bright DNA-Ag NCs template due to higher affinity. Distinctive from the NCB based on G-rich sequence, this transformation occurred no matter when the two DNA templates lay on the same sides or the opposite sides of the duplexes, endowing the NCB design more flexible. And surprisingly, it showed a much better transformation efficency when the two templates approached by the opposite sides of the duplexes. Then this sensing platform was successfully extended to three-strand transformation. The efficiency was as high as 70-fold enhancement when the two templates were on the opposite sides of the duplexes, which was much better than the conventional molecular beacon probes. Additionally, we demonstrated NCB detection of the normal Homo sapiens hemoglobin beta chain gene (HBB) with good sensitivity and selectivity.

Template *a* (5'-CCCTTAATCCCC-3') is a low quantum yield template for Ag NCs with smaller than 6 Ag atoms,[10] whereas template *b* (C_{12}) is demonstrated to be an effective template for bright red emission Ag NCs with 2-7 Ag atoms.[16] When the dark Ag NCs approached to template C_{12} through hybridization, a conspicuous enhancement of fluorescence was observed. Fig. 1A showed two typical hybridizing models of two-strand template transfer. Strand s-a5' was in conjunction with a weak Ag NCs template sequence (*a*) and a 13-base stem for hybridization. Strand s-b3' and s-b5' both had a sequence complementary to the hybridizing part in s-a5' and a C_{12}

[a] State Key Laboratory of Electroanalytical Chemistry, Changchun Institute of Applied Chemistry, Chinese Academy of Sciences, Changchun, Jilin, 130022, China.
[b] University of the Chinese Academy of Sciences, Beijing, 100049, China.
E-mail: ekwang@ciac.ac.cn; Fax: +86-431-85689711; Tel: +86-431-85262003
Electronic Supplementary Information (ESI) available: [details of any supplementary information available should be included here]. See DOI: 10.1039/x0xx00000x
‡ These two authors contributed equally to this work.

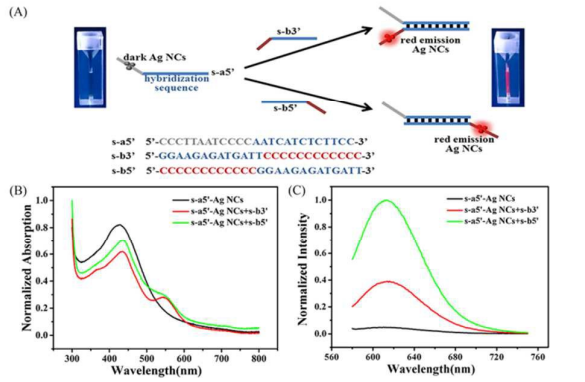

Fig. 1. (A)The schematic demonstration of two typical hybridizing models of two-strand template transfer. (B) UV-Vis absorption and (C) fluorescence spectra of s-a5'-Ag NCs, s-a5'-Ag NCs+s-b3' and s-a5'-Ag NCs+s-b5'.

template (*b*). The only difference was the template position on 3' end or 5' end, which decided the way that two templates approached. Both the two constructions could achieve the transformation of Ag NCs from template *a* to template *b* according to the UV-Vis absorption and fluorescence spectra. In Fig. 1B, there was only an absorption peak at 420 nm in s-a5'-Ag NCs solution, attributing to the surface plasmon resonance peak of larger Ag nanoparticles.[17] After hybridization with s-b3' or s-b5', a shoulder peak at 550 nm appeared. Simultaneously, the fluorescence spectra (Fig. 1C) exhibited that the Ag NCs transferred from dark s-a5'-Ag NCs to bright red emission clusters, leading to 12-fold and 30-fold increase in cluster brightness at 610 nm for s-b3' and s-b5' respectively. To our surprise, the two-end pattern yielded more efficient cluster transfer than the same-end pattern, which was 2.5 times higher in the emission intensity. Moreover, the lifetime measurement of s-a5'-Ag NCs and the transferred Ag NCs presented to be 2.21 ns and 1.95 ns respectively, fitting with a monoexponential function (Fig. S1). The different lifetimes illustrated that the species of Ag NCs had changed after hybridization, leading to the transformation of optical properties.

As control, a complementary sequence without C_{12} template (cs) and a non-hybridized C_{12} template (n-b3') were investigated (Fig. S2). After hybridizing with cs, the fluorescence intensity of s-a5'-Ag NCs had almost no enhancement, indicating that the red emissive fluorescence didn't simply originate from the DNA hybridization of the stem part. The addition of n-b3' strand also led to no obvious enhancement of the fluorescence at 610 nm, indicating that the hybridization was an essential requirement for such template transformation. The possible transfer mechanism was surmised that the hybridization pulled the two templates close to each other, and the C_{12} template captured Ag NCs from the weak template presumably due to the higher specific affinity,[18] concomitant with striking fluorescence intensity enhancement.

The template transformation of DNA-Ag NCs was a general phenomenon to different templates. Taking template *c* (5'-CCCACCCACCCGCCCA-3') as an example, it was a common template for near-infrared emission DNA-Ag NCs (712 nm/ 760 nm).[19] Dark s-a5'-Ag NCs turned to a strong emission at 760 nm after hybridizing with strand s-c5' (Fig. S4). The generality of the template transformation of DNA-Ag NCs showed great potential for multi-detection with different emissive Ag NCs.

The template transformation system was further enlarged to three strands hybridization. Fig. 2A illustrated the schematic of four kinds of hybridization patterns and the sequences we used. Sequences with weak template *a* and strong template *b* were utilized for the investigation (listed in Table S1), and the concentrations of these sequences were all 0.5 μM. The two template strands both had a stem hybridized with the linker strand, making them in proximity to each other through hybridization. In pattern A, the two templates lay on the two ends of the hybridization strands. Pattern B and C were two situations that one template in the middle and the other on the end of hybridization strands. In pattern D, the two templates met in the middle of the hybridization strands. The comparisons of fluorescence enhancement ratio were shown as bar diagrams in Fig. 2B. All the four patterns effectively transferred dark Ag NCs to bright C_{12}-Ag NCs. Notably, pattern A exhibited the best transfer efficiency, a 70 fold enhancement emission. The other three patterns brought approximately 20-30 fold enhancement emission. Similar to two-strand template transfer, the two-end pattern yielded the most effective clusters transfer in the mode of three strands hybridization. The possible underlying reason might be the steric hindrance

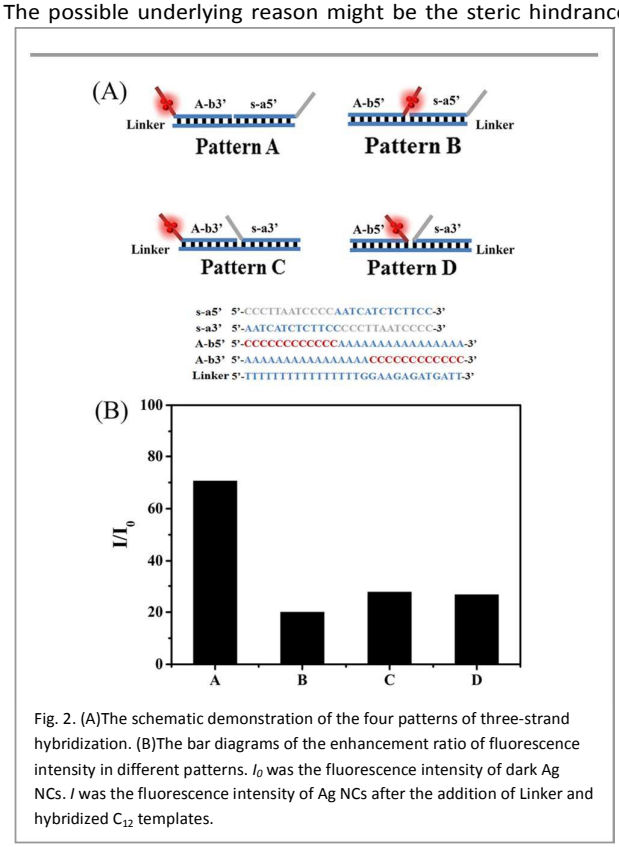

Fig. 2. (A)The schematic demonstration of the four patterns of three-strand hybridization. (B)The bar diagrams of the enhancement ratio of fluorescence intensity in different patterns. I_0 was the fluorescence intensity of dark Ag NCs. *I* was the fluorescence intensity of Ag NCs after the addition of Linker and hybridized C_{12} templates.

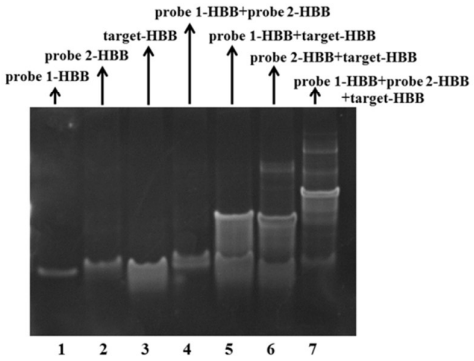

Fig. 3. Native 15% polyacrylamide gel analysis of the hybridization in three-strand template transfer. The DNA strands were added as the description above each lane. The concentrations of DNA were all 2 μM.

and the complicated secondary structure of DNA strands when two templates approached.

To understand deeply about the process of template transformation, we further studied the model of pattern A (s-a5'-Linker-A-b3'). The UV-Vis absorption and fluorescence spectra were shown in Fig. S5. In the presence of Linker, the UV-Vis absorption and fluorescence both greatly increased for the transformation of bright C_{12}-Ag NCs in quantity. Subsequently a toehold sequence of 6 bases was designed to add to the 5' end of Linker (Linker-6). As shown in Fig. S6, after hybridized with Linker-6, s-a5'-Ag NCs were transferred to C_{12} template in A-b3', leading an obvious fluorescence enhancement at 610 nm. Then the completely complementary strand of Linker-6 (Linker-6-co) was added to displace the connecting strand Linker-6. The hybridization of Linker-6 and Linker-6-co made s-a5' and A-b3' separate, but the fluorescence had no decrease. It indicated that the procedure of this template transformation was irreversible，different from the previous G-rich sequence enhancement Ag NCs emission.[11]

To demonstrate the generality of this transformation, the NCB design was used for disease DNA detection. A 24-base segment (target-HBB) of HBB was chosen as the target sequence. The detailed designs of probe sequences, based on the pattern A in three-strand hybridization, were listed in Table S1. In the presence of target DNA, the three strands hybridized, and pulled the two templates approaching on the opposite sides of duplex. The dark Ag NCs transferred from the template part of probe 1-HBB to probe 2-HBB, accompanied with strikingly enhanced fluorescence.

Native polyacrylamide gel electrophoresis (PAGE) was further used to identify the hybridization of these three strands. As shown in Fig. 3, lanes 1-3 were corresponding to three kinds of single strands respectively. Lane 4 was the mixture of probe 1-HBB and probe 2-HBB, which could not hybridize with each other in the absence of target-HBB. Lane 5 and 6 were probe 1-HBB and probe 2-HBB which reacted with target-HBB respectively. Lane 7 was the mixture of all these three strands. Comparing these lanes, both probe 1-HBB and probe 2-HBB could partly hybridize with target DNA, but they could not hybridize with each other without target DNA. In the presence of target DNA, these three strands would hybridize together, forming duplexes as pattern A depicted in Fig. 2. Comparing the result of PAGE with corresponding fluorescence spectra, it was also a further demonstration that hybridization was essential for the template transformation.

Taking the advantage of three-strand template transfer, a simple NCB platform was designed for the detection of gene target-HBB. Under the optimized condition, the linear range of this NCB sensing platform was investigated. As shown in Fig. 4A, the fluorescence intensity increased with the concentration of target-HBB. At low concentrations, the fluorescence intensity grew slowly. However, when the concentration of target-HBB reached 200 nM, there was an obvious rise of the slope. When the target was more than 400 nM, the fluorescence didn't have evident enhancement any more. Finally, two linear relationships were found between fluorescence intensity and target-HBB concentration (Fig. 4B). The linear ranges were 5.0 nM-200 nM (R^2=0.973) and 200 nM-400 nM (R^2=0.974), with the detection limit of 0.5 nM.

The selectivity of DNA variation was then investigated (Fig. 4C). Sequence M1 was the single-nucleotide variation of target-HBB, responsible for sickle cell disease. Sequences M2, M3 and M4 were the strands that had 2, 3 and 4 bases variation respectively comparing with target-HBB. Sequence N was an irrelative gene sequence to target. As shown in Fig. 5C, our

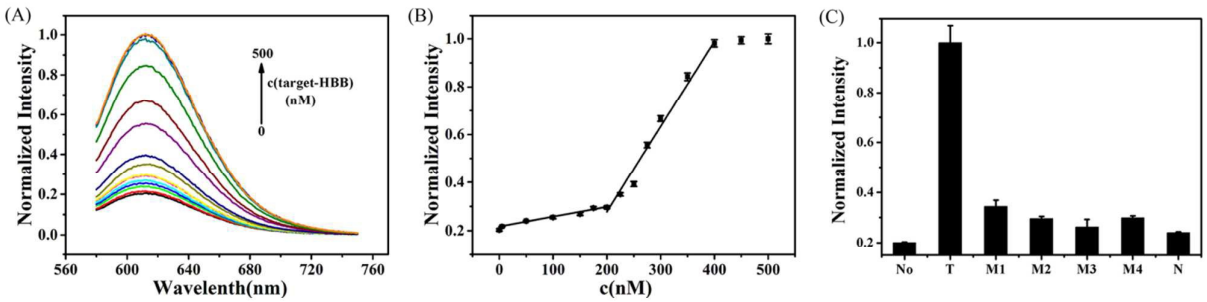

Fig. 4. (A) The fluorescence spectra of 500 nM probe 1-HBB-Ag NCs and probe 2-HBB with different concentration of target DNA. (B) The linear relationship between target concentration and fluorescence intensity. (C) The selectivity of this sensing platform. Sequences M1-M4 had 1-4 base variations to target DNA, respectively. N was an irrelative gene sequence to target DNA.

method could distinguish the variation of target DNA, even single-nucleotide variation, with a good selectivity.

In conclusion, we have demonstrated a new NCB system involving template transformation of Ag NCs through DNA hybridization. This template transfer occurred no matter the two templates lay on the same sides or the opposite sides of the duplexes, and two-end pattern showed a better transfer efficiency. Utilizing this sensing strategy, a simple turn-on fluorescence platform was designed for the detection of disease DNA with good sensitivity and selectivity. This novel NCB is versatile, endowing the biosensor design more flexible, and we look forward for its application on a broader class of targets.

This work is supported by the National Natural Science Foundation of China with Grants 21190040.

Notes and references

1 E. R. Mardis, *Trends Genet.*, 2008, **24**, 133-141.
2 D. Altshuler, M. J. Daly and E. S. Lander, *Science*, 2008, **322**, 881-888.
3 S. Tyagi and F. R. Kramer, *Nat Biotech*, 1996, **14**, 303-308.
4 B. Han and E. Wang, *Anal. Bioanal. Chem.*, 2012, **402**, 129-138.
5 X. Liu, F. Wang, R. Aizen, O. Yehezkeli and I. Willner, *J. Am. Chem. Soc.*, 2013, **135**, 11832-11839.
6 L. Zhang, J. Zhu, S. Guo, T. Li, J. Li and E. Wang, *J. Am. Chem. Soc.*, 2013, **135**, 2403-2406.
7 P. Shah, A. Rorvig-Lund, S. Ben Chaabane, P. W. Thulstrup, H. G. Kjaergaard, E. Fron, J. Hofkens, S. W. Yang and T. Vosch, *ACS Nano*, 2012, **6**, 8803-8814.
8 J. Yin, X. He, K. Wang, Z. Qing, X. Wu, H. Shi and X. Yang, *Nanoscale*, 2012, **4**, 110-112.
9 J. Yin, X. He, K. Wang, F. Xu, J. Shangguan, D. He and H. Shi, *Anal. Chem.*, 2013, **85**, 12011-12019.
10 C. I. Richards, S. Choi, J. C. Hsiang, Y. Antoku, T. Vosch, A. Bongiorno, Y. L. Tzeng and R. M. Dickson, *J. Am. Chem. Soc.*, 2008, **130**, 5038-5039.
11 J. S. Martinez, H. C. Yeh, J. Sharma, J. J. Han and J. H. Werner, *Nano Lett.*, 2010, **10**, 3106-3110.
12 S. Y. Lee, N. H. H. Bahara, Y. S. Choong, T. S. Lim and G. J. Tye, *J. Colloid Interface Sci.*, 2014, **433**, 183-188.
13 X. Tian, X. Kong, Z. Zhu, T. Chen and X. Chu, *Talanta*, 2015, **131**, 116-120.
14 M. Zhang, S. Guo, Y. Li, P. Zuo and B. Ye, *Chem. Commun.*, 2012, **48**, 5488-5490.
15 H.-C. Yeh, J. Sharma, I.-M. Shih, D. M. Vu, J. S. Martinez and J. H. Werner, *J. Am. Chem. Soc.*, 2012, **134**, 11550-11558.
16 C. M. Ritchie, K. R. Johnsen, J. R. Kiser, Y. Antoku, R. M. Dickson and J. T. Petty, *J. Phys. Chem. C*, 2007, **111**, 175-181.
17 J. Zheng and R. M. Dickson, *J. Am. Chem. Soc.*, 2002, **124**, 13982-13983.
18 J. H. Yu, S. Choi and R. M. Dickson, *Angew. Chem., Int. Ed.*, 2009, **48**, 318-320.
19 Y. Teng, X. Yang, L. Han and E. Wang, *Chem.-Eur. J.*, 2014, **20**, 1111-1115.